


Research Article

Increased discharge of Yellow River sediments into the western Bohai Sea since 0.71 Ma

Xin Zhang^{a,b}, Baojing Yue^{a,b*} , Jian Liu^{a,b}, Tianyuan Chen^c, Junqiang Zhang^d and Yuhui An^e

^aQingdao Institute of Marine Geology, Qingdao, 266071, China; ^bLaboratory for Marine Geology, Qingdao National Laboratory for Marine Science and Technology, Qingdao, 266061, China; ^cKey Laboratory of Salt Lake Geology and Environment of Qinghai Province, Qinghai Institute of Salt Lakes, Chinese Academy of Sciences, Xining, 810008, China; ^dInstitute of Geology and Paleontology, Linyi University, Linyi, 276005, China and ^eCollege of Marine Geosciences, Ocean University of China, Qingdao, 266100, China

Abstract

The Yellow River originates on the Tibetan Plateau and transports vast amounts of terrestrial sediment to the ocean. However, previous studies have not reached a consensus as to when and how the Yellow River first began to flow into the sea. Here we present Sr-Nd-Pb isotope data and a high-resolution clay mineral record of a 200-m-long sediment core recovered from the modern Yellow River delta. The changes in Sr-Nd-Pb isotopic compositions and clay minerals at 0.71 Ma suggest that a larger proportion of sediment was derived from the Yellow River after this time. We propose that the Yellow River has influenced the Bohai Sea since 1.9 Ma (or even earlier), which provides important evidence for an older Yellow River than 1.2 Ma. A significant increase in discharge of Yellow River sediments since 0.71 Ma is due to continuing subsidence of the eastern China coast, the large amplitude of Quaternary sea-level changes, and increased supply of eroded loess during the last 1.0 Ma. After this time, the contribution of local rivers surrounding the Bohai Sea became negligible due to dilution by the huge amounts of Yellow River sediments. These results provide improved constraints on the evolution of the Yellow River and subsequent land-sea fluxes.

Keywords: Yellow River, Clay minerals, Sr-Nd-Pb isotopes, Sediment provenance, Sanmen Gorge, Bohai Sea

(Received 22 December 2021; accepted 7 November 2022)

INTRODUCTION

Coastal areas connect the continents and oceans where sedimentation is controlled by the interaction of monsoonal, fluvial, and marine processes (Dalrymple and Choi, 2007; Clift and Jonell, 2021). Over geological time, global climate change, sea-level fluctuations, and terrestrially derived sediment input are recorded by the stratigraphy preserved in these areas (Clift, 2006). Therefore, detailed studies of the sediments deposited at continental margins can provide a better understanding of paleoclimatic and paleoenvironmental changes, as well as the evolution of large rivers (e.g., Miller et al., 2005; Parham et al., 2012; Ridente et al., 2012; McCarthy et al., 2013; Liu et al., 2016; Yao et al., 2017).

The Yellow River is one of the largest rivers in the world (Qin et al., 1990), and has attracted significant scientific interest due to its ecological and economic importance. Numerous studies have investigated the evolution of the Yellow River (e.g., Clark et al., 2004; Liu and Sun, 2007; Kong et al., 2014; Zhang et al., 2019; Xiao et al., 2020, 2021). Nevertheless, the precise age of the final emergence of the Yellow River to the ocean, and its effect on the marginal sea are unclear. For example, fluvial terraces of

the Sanmen Gorge suggest that integration of the Yellow River occurred in the Early Pleistocene (e.g., Pan et al., 2005; Kong et al., 2014; Hu et al., 2019; Liu, 2020). It is noteworthy that the sedimentary sequence of DR01 core in the Hetao Graben indicates that there was an ancient Yellow River at least since 1.7 Ma (Li et al., 2017). Through consideration of the similarity in the sedimentary facies throughout the DR01 core and sedimentary characteristics of the Neogene conglomerates along the Jinshaan Gorge, the Yellow River may have existed at least since the late Neogene (Xiong et al., 2022), which is much earlier than 1.7 Ma. In addition, an abrupt increase in the rate of accumulation of loess deposits in the Mangshan section and the drying up of the Sanmen paleolake are observed and interpreted to indicate downcutting of the Sanmen Gorge and full development of the Yellow River at 0.24–0.15 Ma (Jiang et al., 2007). This large range of ages may reflect the complexity of Yellow River evolution, which needs further investigation.

After the final integration of the Yellow River, the mouth of the Yellow River has moved several times between the Bohai and Yellow seas (Ren and Shi, 1986; Ren, 2015). Provenance analysis of sediments deposited in coastal areas may provide insights into the effects of the Yellow River on the marginal seas of China. Radiogenic Sr, Nd, and Pb isotopes have been used extensively as tracers of sediment sources (e.g., Parra et al., 1997; Choi et al., 2007; Jiang et al., 2019). Although the Sr isotope data are influenced by grain size, Nd isotopes are largely unaffected by mineral sorting and grain size (Chen et al., 2007). Clay minerals are also

*Corresponding author email address: <31417649@qq.com>

Cite this article: Zhang X, Yue B, Liu J, Chen T, Zhang J, An Y (2023). Increased discharge of Yellow River sediments into the western Bohai Sea since 0.71 Ma. *Quaternary Research* 113, 182–190. <https://doi.org/10.1017/qua.2022.64>

sensitive to climate change and can reveal the paleogeographic and stratigraphic history of depositional sequences (Biscaye et al., 1997; Thiry, 2000). Provenance analyses of sediments in the Bohai and South Yellow seas have shown that sediment provenance has been dominated by the Yellow River since 0.9–0.8 Ma (Yao et al., 2017; Zhang et al., 2019). However, single-grain zircon ages from three well-dated late Miocene–Pleistocene boreholes in the lower Yellow River floodplain suggest that the upstream and downstream parts of the Yellow River were connected between 1.6–1.5 Ma (Xiao et al., 2020). This is also supported by detrital zircon U–Pb geochronology and geochemical signals from borehole G4 in the Bohai bay, which show the Yellow River entered the Bohai Bay since ca. 1.6 Ma (Yang et al., 2022). Yet it is noteworthy that zircon can survive multiple cycles of sediment recycling because of its erosion resistance, and therefore may not always represent the most recent phase of sediment transport (Bird et al., 2020). Furthermore, forcing mechanisms for the final integration of the Yellow River are still debated, including climate-driven lake expansion (Craddock et al., 2010; Yao et al., 2017), tectonic processes (Lin et al., 2001; Zhang et al., 2019), and fluvial erosion triggered by Plio–Pleistocene base level fluctuations (Xiao et al., 2020). Therefore, detailed provenance studies of coastal areas of eastern China constrained by precise age models are essential for the timing and mechanism of the final emergence of the Yellow River.

In this study, a 200-m-long core (YRD-1101) was recovered from the modern Yellow River delta on the southwest coast of Bohai Sea. The heavy mineral assemblages in this core (i.e., the epidote to hornblende ratio) revealed that the Yellow River first flowed into the modern Yellow River delta at ca. 0.83 Ma (Liu et al., 2020). However, the relative abundances of heavy minerals are strongly affected by the hydrodynamic conditions during sediment transport (Morton and Hallsworth, 1999), which limit their ability to constrain the sediment provenance. Given the complexity of the evolution of the Yellow River, more studies of sedimentary records around the Bohai Sea are needed. In this regard, we focused on temporal variations in grain size, clay mineral assemblages, and Sr–Nd–Pb isotopes of the <63 µm silicate sediment fraction in the YRD-1101 core. These data provide new evidence for provenance changes during the last ca. 1.9 Ma.

REGIONAL SETTING

The Bohai Sea comprises the Liaodong Bay, Bohai Bay, Laizhou Bay, Central Basin, and Bohai Strait, with a total area of 78,000 km². The average water depth and slope are 18 m and 0.0078°, respectively (Qin et al., 1990). Water enters the Bohai Sea through the northern Bohai Strait and flows out along the southern margin of the Bohai Sea. Circulation in Liaodong Bay forms a clockwise gyre in winter, and counterclockwise gyre in summer (Dou et al., 2014). The tidal regime in the Bohai Sea is dominated by semi-diurnal tides (Qin et al., 1990).

The Yellow River is the second longest river in China, with an estimated length of 5464 km and a watershed area of 7,520,000 km². It originates in the southern part of Qinghai Province on the Tibetan Plateau and crosses the dry Loess Plateau of North China as it flows towards the Bohai Sea. It was estimated that the Yellow River delivered 1.1×10^9 ton/yr of sediment to the sea (Milliman et al., 1987), with 43% of that deposited in the delta (Milliman and Meade, 1983). However, the sediment load has decreased abruptly to 1.5×10^8 tons/year over the last 20 years because of natural and anthropogenic changes (Wang et al., 2007). When the Yellow River changed its course from the South Yellow Sea to the Bohai Sea, the modern Yellow River delta (118.0–119.5°E, 37.0–38.5°N) was formed (Liu et al., 2009; Ren, 2015). The modern Yellow River delta, which has prograded seaward by >40 km in the last 150 yr, presently has an area of ~5000 km² (e.g., Liu et al., 2009; Hu et al., 2012).

In addition to the Yellow River, the Bohai Sea also has received sediment from other small rivers (Fig. 1). The Luan River, which is 877 km long (He et al., 2020), originates from Bayan Tugur Mountain and flows to the sea through the Inner Mongolia Plateau and Yanshan Mountains. The length and drainage area of the Liao River are 1400 km and 220,000 km², respectively (Milliman and Farnsworth, 2011). The Hai River system, including the Yongding River, Daqing River, and Ziya River, has a drainage area of 210,000 km² and discharged more than 8.0×10^6 ton/yr sediments to the Bohai Sea before the 1950s (Qin et al., 2021). Furthermore, the sediment discharge of the Daling (1.77×10^7 ton/yr) and Xiaoling (2.24×10^6 ton/yr) rivers is also significant, although both are small scale in terms of their lengths and catchment areas (Qin et al., 2021).

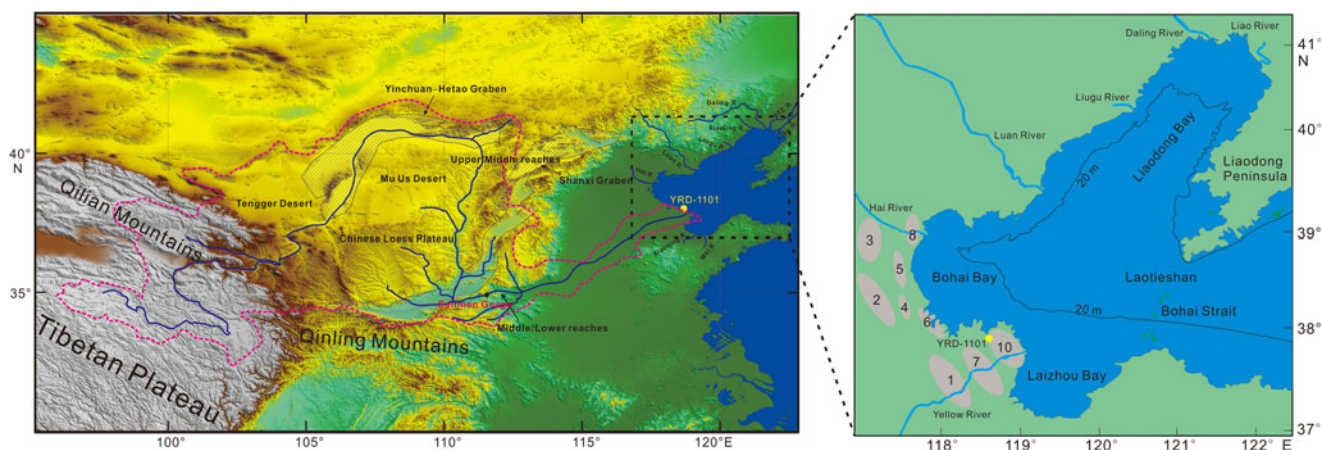


Figure 1. Location of the Yellow River and study area. Dashed red line indicates the Yellow River's drainage area, including its tributaries and the locations mentioned in the text. The gray areas (numbered 1–8, 10, from oldest to youngest) represent nine superlobes formed in the west coast of the Bohai Sea since the Holocene (the superlobe represented by gray area 9 is not shown because it is located in northern Jiangsu Province rather than in the study area). Left side of Figure 1 is modified from Nie et al. (2015).

MATERIALS AND METHODS

The YRD-1101 core (38°02′08.97″N, 118°36′25.88″E; length 200.30 m) was drilled in the modern Yellow River delta using the rotary method in July 2011 (Fig. 1). The core had a mean recovery of 85%. The lithological characteristics show that the core is dominated by fluvial, tidal-flat, littoral, and coastal deposits (Liu *et al.*, 2016). The chronological framework of the core was established by magnetostratigraphy, seven accelerator mass spectrometry (AMS) ^{14}C dates, and 20 optically stimulated luminescence (OSL) dates (Sun *et al.*, 2014; Liu *et al.*, 2016). Paleomagnetic analyses show that the upper boundary of the Jaramillo subchron was at 136.21 m, and the Brunhes/Matuyama (B/M) chron boundary was at 123.33 m (Liu *et al.*, 2016). The age model was constrained by these control points and linear extrapolations of the sedimentation rates. The basal age of YRD-1101 core was estimated to be ca. 1.9 Ma by the upper boundary of the Olduvai subchron at 191.78 m and extrapolation of the average sedimentation rate of 70 m/Ma (i.e., 0.07 m/ka; from 191.78–136.21 m in Figure 2).

In this study, 377 samples were selected for clay mineral analysis. For sample pre-treatment, organic and carbonate phases were removed with 10% H_2O_2 and 0.5 M HCl, respectively. The clay fractions (<2 μm) were extracted and transferred to two slides by wet smearing and then air-dried. Clay minerals were identified by X-ray diffraction (XRD) with a Rigaku D/max-2500 diffractometer using $\text{Cu-K}\alpha$ radiation (40 kV and 100 mA) at the Qingdao Institute of Marine Geology, Qingdao, China. The relative percentages of clay minerals were calculated following the methods of Biscaye (1965) and Biscaye *et al.* (1997), with an error of $\pm 8\text{--}10\%$.

Thirty-four samples of the <63 μm silicate fraction were selected for Sr-Nd-Pb isotope analysis at the Key Laboratory of Marine Sedimentology and Environmental Geology, First

Institute of Oceanography, State Oceanic Administration, Qingdao, China. Prior to analysis, the samples were treated with HCl and H_2O_2 and then digested in high-pressure Teflon bombs using a $\text{HCl} + \text{HNO}_3 + \text{HClO}_4 + \text{HF}$ solution. The Sr and Nd isotope ratios were determined with a Nu Plasma high-resolution inductively coupled plasma mass spectrometer after Sr and Nd separation. Lead was separated using successive acid elution on an anion exchange resin (AG1-X8) column. The separation and analysis of Pb isotopes were undertaken using the methods of Hu *et al.* (2012). Analytical precision of the Sr, Nd, and Pb isotope data were monitored by analysis of the standards NBS 987 ($^{87}\text{Sr}/^{86}\text{Sr} = 0.710310 \pm 0.00003$), JNdi-1 ($^{143}\text{Nd}/^{144}\text{Nd} = 0.512115 \pm 0.000007$), and NIST SRM 981 ($^{208}\text{Pb}/^{204}\text{Pb} = 36.674 \pm 0.004$, $^{207}\text{Pb}/^{204}\text{Pb} = 15.486 \pm 0.003$, and $^{206}\text{Pb}/^{204}\text{Pb} = 16.933 \pm 0.003$; 2σ), respectively. Neodymium isotope data are expressed as $\epsilon\text{Nd} = [({}^{143}\text{Nd}/{}^{144}\text{Nd}_{\text{sample}})/({}^{143}\text{Nd}/{}^{144}\text{Nd}_{\text{CHUR}}) - 1] \times 10,000$, where the CHUR (i.e., the chondritic uniform reservoir) value is 0.512638 (Jacobsen and Wasserburg, 1980).

RESULTS

Clay mineralogy

In the YRD-1101 core, illite (37.0–79.1%) is the dominant clay mineral, with an average percentage of 55.6%. Smectite (0–43.4%; average = 11.2%), kaolinite (8.7–22.2%; average = 14.5%), and chlorite (9–30%; average = 18.7%) are present in the samples in lesser amounts. Down-core variations in the clay mineral assemblage are shown in Figure 2. Smectite and kaolinite contents decrease slightly from bottom to top of the core, whereas illite exhibits the opposite trend.

From 200.30–119.00 m, the relative percentages of illite show an increasing pattern generally, and the trends in kaolinite contents are similar to chlorite, which fluctuate slightly and are

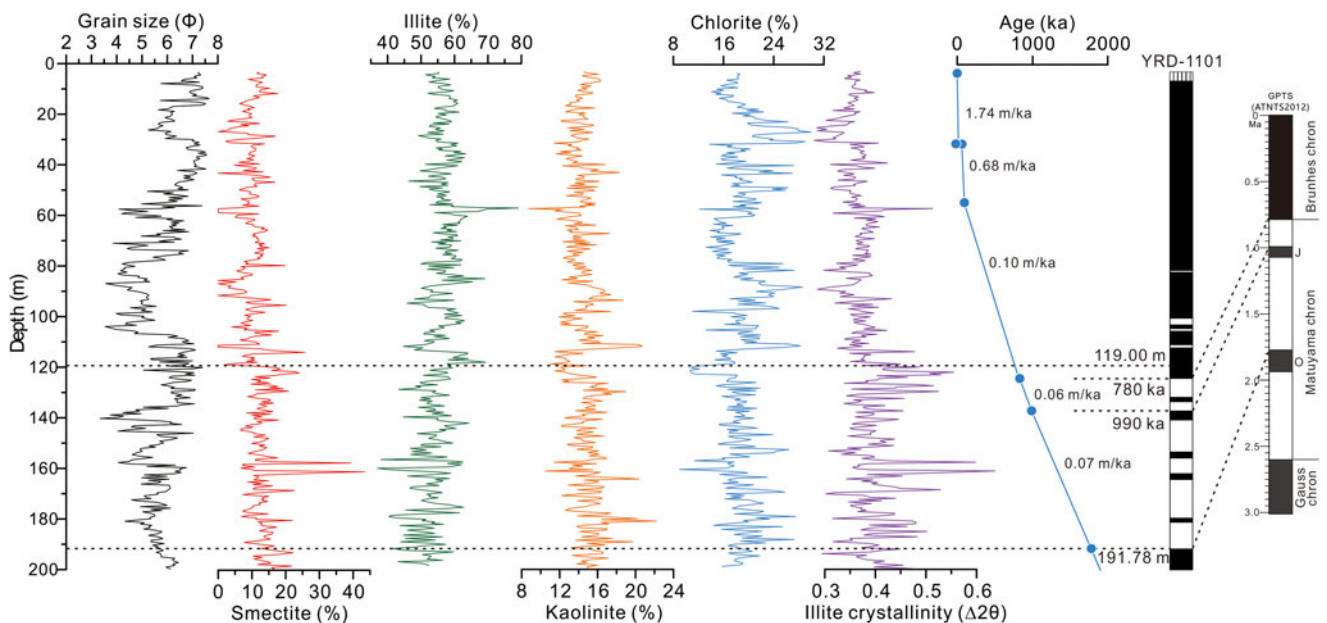


Figure 2. Variations in clay mineral assemblage, illite crystallinity, and sediment accumulation rate in the YRD-1101 core since 1.9 Ma. The magnetostratigraphy (Liu *et al.*, 2016), Geomagnetic Polarity Timescale (GPTS), and Astronomically Tuned Neogene Time Scale 2012 (ATNTS 2012) (Hilgen *et al.*, 2012) are shown for comparison. The “ka” denotes “kyr B.P.” Dashed black line indicates significant change in provenance at ~119 m core depth. Solid blue line indicates sedimentation rate and solid blue dots indicate reliable ages that were obtained by magnetostratigraphy, AMS ^{14}C , and OSL dating; the age model in core YRD-1101 was constrained by these control points and linear extrapolations of the sedimentation rates.

relatively stable. In addition, the illite crystallinity values, which range from 0.294–0.636, exhibit clear fluctuations around a value of 0.4. In this section, smectite contents show a stable trend overall except for few abnormally high values at ~160 m. Notably, a significant boundary can be identified at a depth of 119.00 m, where the content of smectite decreases from 12.7% to 1.9% and the content of illite increases from 57.8% to 69.3%. In the uppermost 119.00 m, the average content of smectite decreases from 13.6% to 9.6%, while that of illite increases 53.0% to 57.3%. Meanwhile, distinct fluctuations in the clay mineral assemblages are evident, especially for chlorite. Some changes in illite crystallinity values are also observed. The illite crystallinity values overall are relatively low and vary between 0.279–0.513, with most values being <0.4 during this period.

Sr-Nd-Pb isotopic compositions

Down-core variations of the Sr-Nd-Pb isotope ratios are shown in Figure 3 and Supplemental Table S1. $^{87}\text{Sr}/^{86}\text{Sr}$ ratios vary between 0.71555–0.72543 and $^{143}\text{Nd}/^{144}\text{Nd}$ ratios range from 0.511809–0.512107 ($\epsilon\text{Nd} = -16.13$ to -10.36). In addition, $^{208}\text{Pb}/^{204}\text{Pb}$, $^{207}\text{Pb}/^{204}\text{Pb}$, and $^{206}\text{Pb}/^{204}\text{Pb}$ ratios vary from 38.8–40.4, 15.60–15.68, and 18.4–19.2, respectively (Supplemental Table S1). Similar to the clay minerals, a change in these isotope ratios occurs at ~119.00 m.

From 200.30–119.00 m, the ϵNd and Pb isotope ratios ($^{208}\text{Pb}/^{204}\text{Pb}$, $^{207}\text{Pb}/^{204}\text{Pb}$, and $^{206}\text{Pb}/^{204}\text{Pb}$) are relatively low and uniform with limited variation, whereas the $^{87}\text{Sr}/^{86}\text{Sr}$ ratios are reversed. In the uppermost (≤ 119.00 m) part of the core, ϵNd and $^{87}\text{Sr}/^{86}\text{Sr}$ ratios display a long-term increasing trend, and the Pb isotope ratios vary synchronously and exhibit large variations (Fig. 3).

Based on the changes in clay mineral assemblages, illite crystallinity, and Sr-Nd-Pb isotopic compositions, a boundary is

observed at ~119.00 m. The depth of 119.00 m is only 4.33 m above the B/M boundary, and the age at this depth (~119.00 m) is estimated to be ca. 0.71 Ma by extrapolation of the average sedimentation rate of 61 m/Ma (i.e., 0.06 m/ka; from 136.21–123.33 m; Fig. 2).

DISCUSSION

Variations in sediment sources in the YRD-1101 core

Knowledge of the potential sediment sources is necessary to assess the sediment provenance in the YRD-1101 core. Due to heavy rainfall and intense human activities, the Yellow River and some other small rivers contribute large amounts of sediment to the Bohai Sea, which has a large effect on the sedimentary system in the coastal-shelf areas of eastern China. Compared with the Yellow River, the other small rivers around the Bohai Sea (e.g., the Hai, Daling, and Liao rivers) discharge a combined average of 7.5×10^7 ton/yr of sediment (Qin et al., 2021). At present, the sediments in the modern Yellow River delta are mainly supplied by the Yellow River (Liu et al., 2009), with minor amounts of sediment delivered from local rivers, such as the Hai, Xiaoqing, and Wei rivers (Fig. 1).

Given the unique mineralogical and geochemical signatures of these potential sources, Sr-Nd isotopic compositions of detrital sediment fractions can reliably trace and be used to identify changes in sediment provenance (e.g., Parra et al., 1997; Choi et al., 2007; Yang et al., 2007; Steinke et al., 2008; Sun and Zhu, 2010; Rao et al., 2015). $^{87}\text{Sr}/^{86}\text{Sr}$ versus $\epsilon\text{Nd}(t)$ is plotted in Figure 4. For comparison purposes, the cited $^{87}\text{Sr}/^{86}\text{Sr}$ and ϵNd data from previously published studies were measured using $<63 \mu\text{m}$ or $<75 \mu\text{m}$ fractions. Unfortunately, Sr-Nd isotope data for other rivers surrounding the Bohai Sea are unavailable. Our data for samples younger than 0.71 Ma overlap those for the modern Yellow River and middle Chinese Loess Plateau (CLP). In

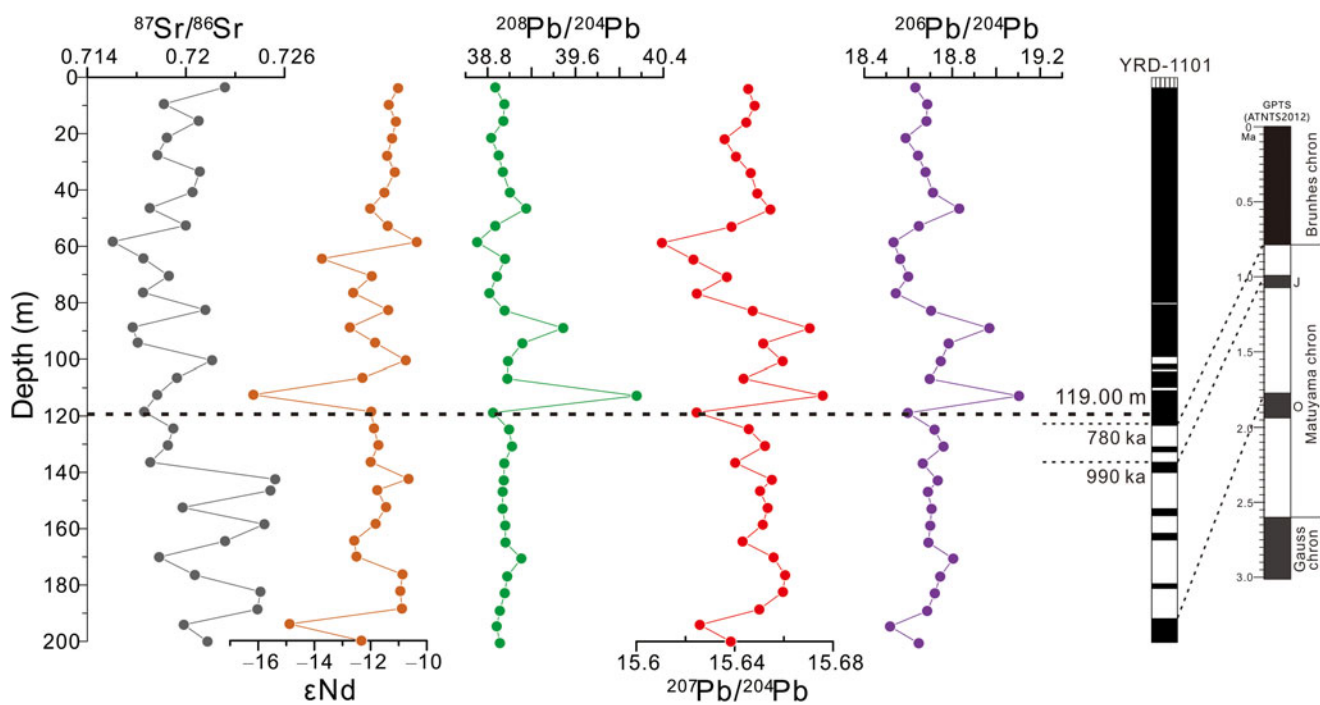


Figure 3. Variations of $^{87}\text{Sr}/^{86}\text{Sr}$, ϵNd , and Pb isotope values in the YRD-1101 core during the last 1.9 Ma.

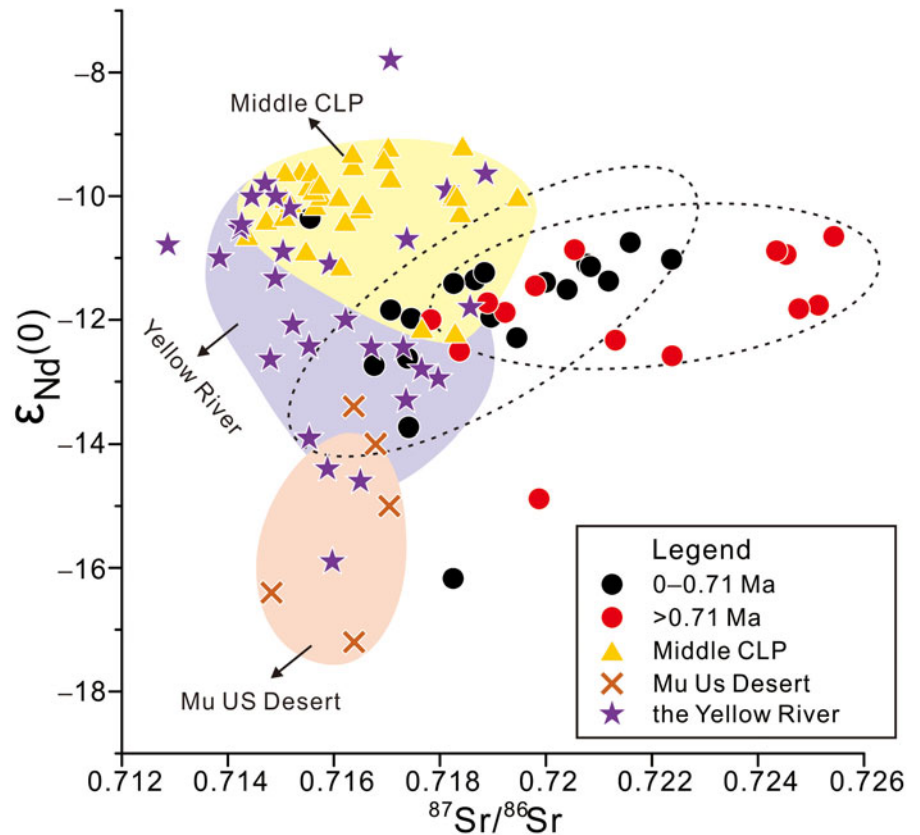


Figure 4. Plot of Sr-Nd isotope data used for sediment provenance discrimination. Also shown are Sr and Nd isotope data for sediments from the Yellow River (Meng et al., 2008; Rao et al., 2011, 2017; Jiang et al., 2019), middle Chinese Loess Plateau (CLP) (Liu et al., 1994; Gallet et al., 1996; Jahn et al., 2001; Chen et al., 2007; W.B. Rao et al., 2008; Yang et al., 2009), and Mu Us desert (W.B. Rao et al., 2008).

contrast, most of our data for samples older than 0.71 Ma deviate to some extent from the Yellow River sediment field, indicating contributions from other sediment sources. In addition, relatively low isotope ratios of Pb, which fluctuate within narrow range of values (Fig. 3), are observed in sediments older than 0.71 Ma. This may be caused by large amounts of multi-sourced sediment inputs, which might have complicated the Pb isotopic compositions (Yao et al., 2017). However, few data are available in previous studies to characterize the potential sources. After that, clear variations in the Pb isotopic ratios are observed in the uppermost 119.00 m (Fig. 3), although this changing tendency is not easy to distinguish due to the low-resolution sampling.

Clay mineral assemblages can provide additional constraints on the sediment provenance and paleoclimatic changes (Ehrmann et al., 2007; Adriaens et al., 2018). Most Yellow River-derived sediments are eroded from the Chinese Loess Plateau (Wang et al., 2007), and the loess deposits have no significant variations in clay mineral composition (Zhang et al., 2019). Figure 5 shows a smectite, (illite + chlorite), kaolinite ternary diagram, on which our data are plotted along with modern river data. Almost all samples younger than 0.71 Ma plot close to the modern Yellow River field. In contrast, samples older than 0.71 Ma plot between the modern Yellow River field and those for some mountainous rivers surrounding the Bohai Sea. Therefore, sediments older than 0.71 Ma were primarily sourced from the Yellow River, but with additions from some local rivers (e.g., the Liao, Wei, Liugu, Daling, and Xiaoling rivers). Similar results have been reported for the sediments in BH08 core (Yao et al., 2017).

Figure 2 shows that the average smectite content decreased from 13.6% to 9.6% at ~119.00 m. Compared with the dominance

of illite in sediments of the Yellow River, the mountainous rivers around the Bohai Sea contain higher smectite contents than the Yellow River (Dou et al., 2014; Yao et al., 2017), indicating the provenance changed from multiple sources to one dominated by the Yellow River. Furthermore, the illite crystallinity values are usually higher (>0.4) in sediments derived from the local rivers (e.g., the Liao, Daling, and Xiaoling rivers) as compared with sediments derived from the Yellow River (Dou et al., 2014). The illite crystallinity values generally vary from 0–0.4 in the upper section (0–119.00 m) and 3.7–5.0 in the lower section (119.00–200.30 m) (Fig. 2). Figure 6 shows a tendency that almost all the samples younger than 0.71 Ma plot in the Yellow River field, although several samples have higher illite crystallinity values (>0.4) and overlap with the sediment field for local rivers. This phenomenon further demonstrates a significant increase in discharge of Yellow River sediments after 0.71 Ma.

Our results suggest that the sediments delivered to the study site were mainly derived from the Yellow River and some local rivers surrounding the Bohai Sea prior to 0.71 Ma. A significant increase in Yellow River sediments delivered to the study area has occurred since ca. 0.71 Ma, when the provenance became dominated by the Yellow River.

Factors driving the provenance changes since 1.9 Ma

The ages and origins of sediments deposited in coastal area of the Bohai Sea are important for constraining the timing and mechanisms of the final emergence of the Yellow River. Based on new detrital-zircon evidence from the North China Plain (Xiao et al., 2020; Yang et al., 2022), coupled with the characteristics of heavy minerals and sedimentary structures of terrace gravel

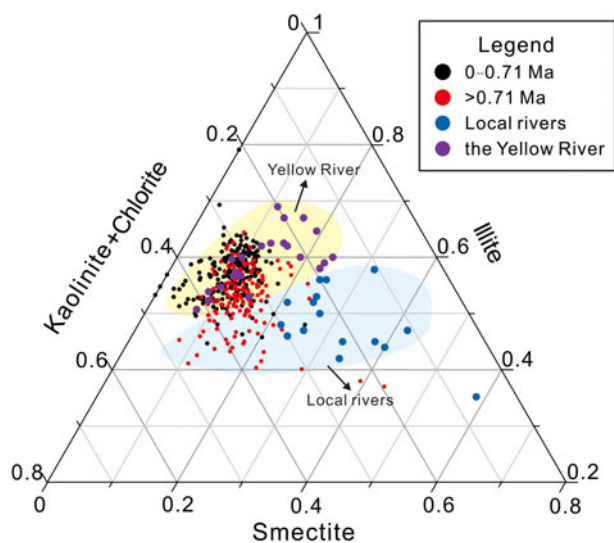


Figure 5. Ternary diagram of smectite, illite, and kaolinite + chlorite contents in the YRD-1101 core. The Yellow River and other local rivers end-member sources of sediment are represented by yellow and blue areas, respectively.

layers along the Yellow River (Hu et al., 2019), current data do not provide support for the hypothesis that full integration of the Yellow River occurred in the late Pleistocene (Jiang et al., 2007; Zheng et al., 2007). This is also supported by geochemical evidence in the CSDP-1 core, which suggests a shift of sediment provenance in the South Yellow Sea from the Yangtze to the Yellow River during 1.7–1.5 Ma (Huang et al., 2021). The clay mineral assemblages and Sr-Nd-Pb isotope record in YRD-1101 core suggest that sediments along the western coast of the Bohai Sea were mainly delivered by the Yellow River and some

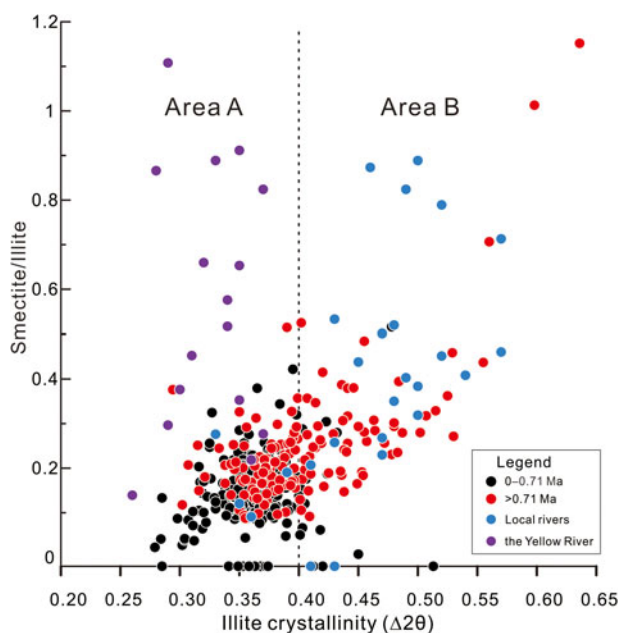


Figure 6. Plot of smectite/illite versus the illite crystallinity for the YRD-1101 core. The sediment sources of the Yellow River and local rivers around the Bohai Sea are represented by Area A and Area B, respectively. Note that almost all the samples younger than 0.71 Ma plot in Area A, although several samples have higher illite crystallinity values (>0.4) and plot in Area B.

local rivers surrounding the Bohai Sea during 1.9–0.71 Ma, implying that the Yellow River may have influenced the Bohai Sea since 1.9 Ma. From a comparative perspective, our new data extend the age of integration of the Yellow River to ever older times.

Geochronology and tectonic geomorphology studies have demonstrated that a recent uplift of the Tibetan Plateau (i.e., Kunlun-Huanghe movement) occurred between 1.2–0.8 Ma (Shi, 1998; Liu and Sun, 2007; Li et al., 2014; Zhang et al., 2017), which has been regarded as the first-order control on integration of the Yellow River sediments (Zhang et al., 2019). However, our data indicate that the Yellow River influenced the Bohai Sea much earlier than 1.2 Ma, implying that the tectonic geomorphological pattern of the Yellow River basin was established prior to the Early Pleistocene.

It is also noted that sediment contribution from the Yellow River has increased significantly since 0.71 Ma in the YRD-1101 core, which provides new insights into the evolution of the Yellow River. Subsidence of the eastern China coast in the past 1.0 Ma was significant, which provides a basis for the generation of accumulation space for influx of sediment (Cosgrove et al., 2022). For instance, previous studies have revealed that seawater entered the Bohai Sea due to accelerated subsidence of the basins in the Bohai and South Yellow seas since ca. 0.83 Ma (Liu et al., 2016, 2018). Sediment loading from the Yellow River, in turn, affects basin subsidence and, consequently, the rate of sediment accumulation.

Additionally, the orbital obliquity cycles of 41 ka were superseded by 100 ka cycles during the Middle Pleistocene Transition (Mudelsee and Schulz, 1997), and stronger climatic oscillations and longer glacial-interglacial cycles developed (Maslin and Brierley, 2015). The amplitude of the 100 ka cycles has generally increased since 0.9 Ma and became largest at ca. 0.7 Ma (Berger et al., 1994). The lowstand sea-level drop during glacial periods also could have induced increased river incision and morphological instability (Gibbard and Lewin, 2009; Head and Gibbard, 2015). Continuous subsidence of the Bohai Basin, along with the sea-level oscillations associated with climate change in the last 1.0 Ma, caused an increase in the fluvial gradient and intensification of sedimentary dynamics (Humphrey and Konrad, 2000; Dauteuil et al., 2015; Yi et al., 2016; Xiao et al., 2020). More importantly, the Quaternary glacial-interglacial cycles and supply of proximal sources also led to the rapid increase in loess sedimentation since ca. 1.0 Ma (Guo et al., 2002; Nie et al., 2015; Xiong et al., 2021), which could be the key reasons for the increase of Yellow River sediments in the Bohai Basin. This is supported by the age-depth curve (Fig. 2), which shows that the rate of sediment accumulation has increased significantly since ca. 0.71 Ma.

In summary, we propose a two-stage evolutionary model for the development of the Yellow River. On the one hand, we hypothesize that the Yellow River has influenced the Bohai Sea since 1.9 Ma (or even earlier). Considering that the Sanmen Gorge may have been shallow and narrow at the early stage of its incision (Xiao et al., 2020), it is unlikely that the Yellow River could have delivered large amounts of sediment to the Bohai Sea. On the other hand, with continuing subsidence of the eastern China coast, large-amplitude sea-level changes, and increased supply of eroded loess during the last 1.0 Ma (Berger et al., 1994; Head and Gibbard, 2015), incision of the Yellow River has intensified. The Sanmen Gorge became deeper and wider, which intensified the delivery of Yellow River sediments into the Bohai Sea. Our data suggest significantly increased

discharge of Yellow River sediments into the study area since 0.71 Ma in YRD-1101, indicating that the contribution of local rivers surrounding the Bohai Sea became negligible due to dilution by the huge amounts of Yellow River sediments. It should be noted that large-scale channel shifting of the Yellow River was observed on the Huabei Plain during the Chinese history (Xue et al., 2003; He et al., 2019), which may have contributed to the possible lag between 1.0 Ma and 0.71 Ma. Interestingly, this significant increase in sediment discharge post-dated the change in the heavy mineral assemblages of the same core (0.83 Ma; Liu et al., 2020). Given that heavy mineral assemblages also can be affected by hydrodynamic conditions during sediment transport (Morton and Hallsworth, 1999), we suggest that the timing of provenance change obtained from the heavy mineral assemblages may be less reliable.

CONCLUSIONS

The Sr-Nd-Pb isotopic composition and clay mineralogy of the YRD-1101 core from the modern Yellow River delta were used to determine the sediment provenance and development of the Yellow River, which leads to two main conclusions. (1) The YRD-1101 core is divided into two intervals with a boundary between the two at 119.00 m (corresponding to an age of 0.71 Ma). Clay mineralogy and Sr-Nd-Pb isotope data for samples overlap those for the modern Yellow River in the upper interval, whereas they deviate to some extent from the Yellow River sediment field in the lower interval. (2) Sediments along the western coast of the Bohai Sea were mainly delivered by the Yellow River and some local rivers surrounding the Bohai Sea during 1.9–0.71 Ma, implying that the Yellow River may have influenced the Bohai Sea since 1.9 Ma. A significant increase in discharge of Yellow River sediments into the study area has occurred since 0.71 Ma, with the provenance now dominated by the Yellow River.

Supplementary Material. The supplementary material for this article can be found at <https://doi.org/10.1017/qua.2022.64>

Acknowledgments. We are grateful to the editors and anonymous reviewers for their constructive comments on our manuscript.

Financial Support. This research was funded by the National Natural Science Foundation of China (Grant No. 41330964) and Natural Science Foundation of Shandong Province, China (Grant No. ZR2020MD069). This research was also funded by the China Geological Survey Projects (Grant No. DD20221724).

REFERENCES

Adriaens, R., Zeelmaekers, E., Fettweis, M., Vanlierde, E., Vanlede, J., Stassen, P., Elsen, J., Śródoń, J., Vandenberghe, N., 2018. Quantitative clay mineralogy as provenance indicator for recent muds in the southern North Sea. *Marine Geology* **398**, 48–58.

Berger, W.H., Yasuda, M.K., Bickert, T., Wefer, G., Takayama, T., 1994. Quaternary time scale for the Ontong Java Plateau: Milankovitch template for Ocean Drilling Program Site 806. *Geology* **22**, 463–467.

Bird, A., Millar, I., Rodenburg, T., Stevens, T., Rittner, M., Vermeesch, P., Lu, H.Y., 2020. A constant Chinese Loess Plateau dust source since the late Miocene. *Quaternary Science Reviews* **227**, 106042. <https://doi.org/10.1016/j.quascirev.2019.106042>.

Biscaye, P.E., 1965. Mineralogy and sedimentation of recent deep-sea clay in the Atlantic Ocean and adjacent seas and oceans. *Geological Society of America Bulletin* **76**, 803–832.

Biscaye, P.E., Grousset, F.E., Revel, M., Van der Gaast, S., Zielinski, G.A., Vaars, A., Kukla, G., 1997. Asian provenance of glacial dust (stage2) in

the Greenland ice sheet project 2 ice core, summit, Greenland. *Journal of Geophysical Research, Oceans* **102**, 26765–26781.

Chen, J., Li, G., Yang, J., Rao, W., Lu, H., Balsam, W., Sun, Y., Li, J., 2007. Nd and Sr isotopic characteristics of Chinese deserts: implications for the provenances of Asian dust. *Geochimica et Cosmochimica Acta* **71**, 3904–3914.

Choi, M.-S., Yi, H.-I., Yang, S.Y., Lee, C.B., Cha, H.-J., 2007. Identification of Pb sources in Yellow Sea sediments using stable Pb isotope ratios. *Marine Chemistry* **107**, 255–274.

Clark, M.K., Schoenbohm, L.M., Royden, L.H., Whipple, K.X., Burchfiel, B.C., Zhang, X., Tang, W., Wang, E., Chen, L., 2004. Surface uplift, tectonics, and erosion of eastern Tibet from large-scale drainage patterns. *Tectonics* **23**, TC106. <https://doi.org/10.1029/2002TC001402>.

Clift, P., 2006. Controls on the erosion of Cenozoic Asia and the flux of clastic sediment to the ocean. *Earth and Planetary Science Letters* **241**, 571–580.

Clift, P.D., Jonell, T.N., 2021. Monsoon controls on sediment generation and transport: mass budget and provenance constraints from the Indus River catchment, delta and submarine fan over tectonic and multimillennial time-scales. *Earth-Science Reviews* **220**, 103682. <https://doi.org/10.1016/j.earscirev.2021.103682>.

Cosgrove, G.I.E., Colombera, L., Mountney, N.P., 2022. The role of subsidence and accommodation generation in controlling the nature of the aeolian stratigraphic record. *Journal of the Geological Society* **179**, jgs2021–042. <https://doi.org/10.1144/jgs2021-042>.

Craddock, W.H., Kirby, E., Harkins, N.W., Zhang, H.P., Shi, X.H., Liu, J.H., 2010. Rapid fluvial incision along the Yellow River during headward basin integration. *Nature Geoscience* **3**, 209–213.

Dalrymple, R.W., Choi, K., 2007. Morphologic and facies trends through the fluvial-marine transition in tide-dominated depositional systems: a schematic framework for environmental and sequence-stratigraphic interpretation. *Earth-Science Reviews* **81**, 135–174.

Dauteuil, O., Bessin, P., Guillocheau, F., 2015. Topographic growth around the Orange River valley, southern Africa: a Cenozoic record of crustal deformation and climatic change. *Geomorphology* **233**, 5–19.

Dou, Y.G., Li, J., Zhao, J.T., Wei, H.L., Yang, S.Y., Bai, F.L., Zhang, D.L., Ding, X., Wang, L.B., 2014. Clay mineral distributions in surface sediments of the Liaodong Bay, Bohai Sea and surrounding river sediments: sources and transport patterns. *Continental Shelf Research* **73**, 72–82.

Ehrmann, W., Schmiedl, G., Hamann, Y., Kuhnt, T., Hemleben, C., Siebel, W., 2007. Clay minerals in late glacial and Holocene sediments of the northern and southern Aegean Sea. *Palaeogeography, Palaeoclimatology, Palaeoecology* **249**, 36–57.

Gallet, S., Jahn, B.-M., Torri, M., 1996. Geochemical characterization of the Luochuan loess-paleosol sequence, China, and paleoclimatic implications. *Chemical Geology* **133**, 67–88.

Gibbard, P.L., Lewin, J., 2009. River incision and terrace formation in the late Cenozoic of Europe. *Tectonophysics* **474**, 41–55.

Guo, Z.T., Ruddiman, W.F., Hao, Q.Z., Wu, H.B., Qiao, Y.S., Zhu, R.X., Peng, S.Z., Wei, J.J., Yuan, B.Y., Liu, T.S., 2002. Onset of Asian desertification by 22 Myr ago inferred from loess deposits in China. *Nature* **416**, 159–163.

Head, M.J., Gibbard, P.L., 2015. Early–middle Pleistocene transitions: linking terrestrial and marine realms. *Quaternary International* **389**, 7–46.

He, L., Xue, C.T., Ye, S.Y., Amorosi, A., Yuan, H.M., Yang, S.X., Laws, E.A., 2019. New evidence on the spatial-temporal distribution of superlobes in the Yellow River Delta Complex. *Quaternary Science Reviews* **214**, 117–138.

He, L., Amorosi, A., Ye, S.Y., Xue, C.T., Yang, S.X., Laws, E.A., 2020. River avulsions and sedimentary evolution of the Luanhe fan-delta system (North China) since the late Pleistocene. *Marine Geology* **425**, 106194. <https://doi.org/10.1016/j.margeo.2020.106194>.

Hilgen, F.J., Lourens, L.J., Van Dam, J.A., 2012. The Neogene Period. In: Gradstein, F.M., Ogg, J.G., Schmitz, M.D., Ogg, G.M. (Eds.), *The Geological Time Scale 2012*. Elsevier BV, Amsterdam, pp. 923–978.

Hu, B.Q., Li, G.G., Li, J., Bi, J.Q., Zhao, J.T., Bu, R.Y., 2012. Provenance and climate change inferred from Sr-Nd-Pb isotopes of late Quaternary sediments in the Huanghe (Yellow River) Delta, China. *Quaternary Research* **78**, 561–571.

- Hu, Z.B., Li, M.H., Dong, Z.J., Guo, L.Y., Bridgland, D., Pan, B.T., Li, X.H., Liu, X.F., 2019. Fluvial entrenchment and integration of the Sanmen Gorge, the Lower Yellow River. *Global and Planetary Change* **178**, 129–138.
- Huang, X.T., Mei, X., Yang, S.Y., Zhang, X.H., Li, F.L., Hohlf, S.V., 2021. Disentangling combined effects of sediment sorting, provenance, and chemical weathering from a Pliocene–Pleistocene sedimentary core (CSDP-1) in the South Yellow Sea. *Geochemistry, Geophysics, Geosystems* **22**, e2020GC009569. <https://doi.org/10.1029/2020GC009569>.
- Humphrey, N.F., Konrad, S.K., 2000. River incision or diversion in response to bedrock uplift. *Geology* **28**, 43–46.
- Jacobsen, S.B., Wasserburg, G.J., 1980. Sm–Nd isotopic evolution of chondrites. *Earth and Planetary Science Letters* **50**, 139–155.
- Jahn, B.M., Gallet, S., Han, J., 2001. Geochemistry of the Xining, Xifeng and Jixian sections, Loess Plateau of China: eolian dust provenance and paleosol evolution during the last 140 ka. *Chemical Geology* **178**, 71–94.
- Jiang, F.C., Fu, J.L., Wang, S.B., Sun, D.H., Zhao, Z.Z., 2007. Formation of the Yellow River, inferred from loess-paleosol sequence in Mangshan and lacustrine sediments in Sanmen Gorge, China. *Quaternary International* **175**, 62–70.
- Jiang, F.Q., Xiong, Z.F., Frank, M., Yin, X.B., Li, A.C., 2019. The evolution and control of detrital sediment provenance in the middle and northern Okinawa Trough since the last deglaciation: evidence from Sr and Nd isotopes. *Palaeogeography, Palaeoclimatology, Palaeoecology* **522**, 1–11.
- Kong, P., Jia, J., Zheng, Y., 2014. Time constraints for the Yellow River traversing the Sanmen Gorge. *Geochemistry, Geophysics, Geosystems* **15**, 395–407.
- Li, B.F., Sun, D.H., Xu, W.H., Wang, F., Liang, B.Q., Ma, Z.W., Wang, X., Li, Z.J., Chen, F.H., 2017. Paleomagnetic chronology and paleoenvironmental records from drill cores from the Hetao Basin and their implications for the formation of the Hobq Desert and the Yellow River. *Quaternary Science Reviews* **156**, 69–89.
- Li, J.J., Fang, X.M., Song, C.H., Pan, B.T., Ma, Y.Z., Yan, M.D., 2014. Late Miocene–Quaternary rapid stepwise uplift of the NE Tibetan Plateau and its effects on climatic and environmental changes. *Quaternary Research* **81**, 400–423.
- Lin, A.M., Yang, Z.Y., Sun, Z.M., Yang, T.S., 2001. How and when did the Yellow River develop its square bend? *Geology* **29**, 951–954.
- Liu, C.Q., Masuda, A., Okada, A., Yabuki, S., Fan, Z.L., 1994. Isotope geochemistry of Quaternary deposits from the arid lands in northern China. *Earth and Planetary Science Letters* **127**, 25–38.
- Liu, J., Saito, Y., Wang, H., Zhou, L., Yang, Z., 2009. Stratigraphic development during the Late Pleistocene and Holocene offshore of the Yellow River delta, Bohai Sea. *Journal of Asian Earth Sciences* **36**, 318–331.
- Liu, J., Wang, H., Wang, F., Qiu, J., Saito, Y., Lu, J., Zhou, L., Xu, G., Du, X., Chen, Q., 2016. Sedimentary evolution during the last ~1.9 Ma near the western margin of the modern Bohai Sea. *Palaeogeography, Palaeoclimatology, Palaeoecology* **451**, 84–96.
- Liu, J., Zhang, J.Q., Miao, X.D., Xu, S.J., Wang, H. X., 2020. Mineralogy of the core YRD-1101 of the Yellow River Delta: implications for sediment origin and environmental evolution during the last ~1.9Myr. *Quaternary International* **537**, 79–87.
- Liu, J., Zhang, X.H., Mei, X., Zhao, Q.H., Guo, X.W., Zhao, W.N., Liu, J.X., et al., 2018. The sedimentary succession of the last ~3.50 Myr in the western South Yellow Sea: Paleoenvironmental and tectonic implications. *Marine Geology* **399**, 47–65.
- Liu, Y., 2020. Neogene fluvial sediments in the northern Jinshaan Gorge, China: implications for early development of the Yellow River since 8 Ma and its response to rapid subsidence of the Weihe-Shanxi Graben. *Palaeogeography, Palaeoclimatology, Palaeoecology* **546**, 109675. <https://doi.org/10.1016/j.palaeo.2020.109675>.
- Liu, Z.J., Sun, Y.J., 2007. Uplift of the Qinghai-Tibet Plateau and formation, evolution of the Yellow River. *Geography and Geo-Information Science* **23**, 79–82. [in Chinese with English abstract]
- Maslin, M.A., Brierley, C.M., 2015. The role of orbital forcing in the early Middle Pleistocene Transition. *Quaternary International* **389**, 47–55.
- McCarthy, F.M.G., Katz, M.E., Kotthoff, U., Browning, J.V., Miller, K.G., Zanatta, R., Williams, R.H., et al., 2013. Sea-level control of New Jersey margin architecture: palynological evidence from Integrated Ocean Drilling Program Expedition 313. *Geosphere* **9**, 1457–1487.
- Meng, X.W., Liu, Y.G., Shi, X.F., Du, D.W., 2008. Nd and Sr isotopic compositions of sediments from the Yellow and Yangtze rivers: implications for partitioning tectonic terranes and crust weathering of the Central and Southeast China. *Frontiers of Earth Science in China* **2**, 418–426.
- Miller, K.G., Kominz, M.A., Browning, J.V., Wright, J.D., Mountain, G.S., Katz, M.E., Sugar, P.J., Cramer, B.S., Christie-Blick, N., Pekar, S.E., 2005. The Phanerozoic record of global sea-level change. *Science* **310**, 1293–1298.
- Milliman, J.D., Farnsworth, K.L., 2011. *River Discharge to the Coastal Ocean: A Global Synthesis*. Cambridge University Press, Cambridge.
- Milliman, J.D., Meade, R.H., 1983. World-wide delivery of river sediment to the oceans. *The Journal of Geology* **91**, 1–21.
- Milliman, J.D., Qin, Y.S., Ren, M.E., Saito, Y., 1987. Man's influence on the erosion and transport of sediment by Asian rivers: the Yellow River (Huanghe) example. *The Journal of Geology* **95**, 751–762.
- Morton, A.C., Hallsworth, C.R., 1999. Processes controlling the composition of heavy mineral assemblages in sandstones. *Sedimentary Geology* **124**, 3–29.
- Mudelsee, M., Schulz, M., 1997. The Middle-Pleistocene climate transition: onset of 100 ka cycle lags ice volume build-up by 280 ka. *Earth and Planetary Science Letters* **151**, 117–123.
- Nie, J.S., Stevens, T., Rittner, M., Stockli, D., Garzanti, E., Limonta, M., Bird, A., et al., 2015. Loess Plateau storage of northeastern Tibetan Plateau-derived Yellow River sediment. *Nature Communications* **6**, 8511. <https://doi.org/10.1038/ncomms9511>.
- Pan, B.T., Wang, J.P., Gao, H.S., Guan, Q.Y., Wang, Y., Su, H., Li, B.Y., Li, J.J., 2005. Paleomagnetic dating of the topmost terrace in Kouma, Henan and its indication to the Yellow River's running through Sanmen Gorges. *Chinese Science Bulletin* **50**, 657–664.
- Parham, P.R., Riggs, S.R., Culver, S.J., Mallinson, D.J., Rink, W.J., Burdette, K., 2012. Quaternary coastal lithofacies, sequence development and stratigraphy in a passive margin setting, North Carolina and Virginia, USA. *Sedimentology* **60**, 503–547.
- Parra, M., Faugeres, J.-C., Grousset, F., Pujol, C., 1997. Sr–Nd isotopes as tracers of fine-grained detrital sediments: the South-Barbados accretionary prism during the last 150 kyr. *Marine Geology* **136**, 225–243.
- Qin, Y., Zhao, Y., Chen, L., Zhao, S., 1990. *Geology of the Bohai Sea*. Science Press, Beijing. [in Chinese]
- Qin, Y.C., Mei, X., Jiang, X.J., Luan, X.W., Zhou, L.Y., Zhu, X.Q., 2021. Sediment provenance and tidal current-driven recycling of Yellow River detritus in the Bohai Sea, China. *Marine Geology* **436**, 106473. <https://doi.org/10.1016/j.margeo.2021.106473>.
- Rao, V.P., Shynu, R., Singh, S.K., Naqvi, S.W.A., Kessarkar, P.M., 2015. Mineralogy and Sr–Nd isotopes of SPM and sediment from the Mandovi and Zuari estuaries: Influence of weathering and anthropogenic contribution. *Estuarine, Coastal and Shelf Science* **156**, 103–115.
- Rao, W.B., Chen, J., Yang, J.D., Ji, J.F., Li, G.J., Tan, H.B., 2008. Sr–Nd isotopic characteristics of eolian deposits in the Erdos Desert and Chinese Loess Plateau: implications for their provenances. *Geochemical Journal* **42**, 273–282.
- Rao, W.B., Chen, J., Tan, H.B., Jiang, S.Y., Su, J., 2011. Sr–Nd isotopic and REE geochemical constraints on the provenance of fine-grained sands in the Ordos deserts, north-central China. *Geomorphology* **132**, 123–138.
- Rao, W.B., Mao, C.P., Wang, Y.G., Huang, H.M., Ji, J.F., 2017. Using Nd–Sr isotopes and rare earth elements to study sediment provenance of the modern radial sand ridges in the southwestern Yellow Sea. *Applied Geochemistry* **81**, 23–35.
- Ren, M., 2015. Sediment discharge of the Yellow River, China: past, present and future—A synthesis. *Acta Oceanologica Sinica* **34**, 1–8.
- Ren, M.E., Shi, Y.L., 1986. Sediment discharge of the Yellow River (China) and its effect on the sedimentation of the Bohai and the Yellow Sea. *Continental Shelf Research* **6**, 785–810.
- Ridente, D., Petrunaro, R., Falase, F., Chiocci, F.L., 2012. Middle–Upper Pleistocene record of 100-ka depositional cycles on the Southern Tuscany continental margin (Tyrrhenian Sea, Italy): sequence architecture and margin growth pattern. *Marine Geology* **326–328**, 1–13.
- Shi, Y.F., 1998. Evolution of the cryosphere in the Tibetan Plateau, China, and its relationship with the global change in the mid Quaternary. *Journal of Glaciology and Geocryology* **20**, 197–208. [in Chinese with English abstract]

- Steinke, S., Hanebuth, T.J.J., Vogt, C., Stattegger, K., 2008. Sea level induced variations in clay mineral composition in the southwestern South China Sea over the past 17,000 yr. *Marine Geology* **250**, 199–210.
- Sun, J.M., Zhu, X.K., 2010. Temporal variations in Pb isotopes and trace element concentrations within Chinese eolian deposits during the past 8 Ma: implications for provenance change. *Earth and Planetary Science Letters* **290**, 438–447.
- Sun, L.S., Liu, J., Qiu, J.D., Li, G.T., Xiang, L.S., 2014. Studies on magnetostratigraphy of core YRD-1101 sediments on the north shore of modern Yellow River Delta. *Marine Geology & Quaternary Geology* **34**, 31–40. [in Chinese with English abstract]
- Thiry, M., 2000. Palaeoclimatic interpretation of clay minerals in marine deposits: an outlook from the continental origin. *Earth-Science Reviews* **49**, 201–221.
- Wang, H.J., Yang, Z.S., Saito, Y., Liu, J.P., Sun, X.X., Wang, Y., 2007. Stepwise decreases of the Huanghe (Yellow River) sediment load (1950–2005): impacts of climate change and human activities. *Global and Planetary Change* **57**, 331–354.
- Xiao, G.Q., Sun, Y.Q., Yang, J.L., Yin, Q.Z., Dupont-Nivet, G., Licht, A., Kehew, A.E., *et al.*, 2020. Early Pleistocene integration of the Yellow River I: detrital-zircon evidence from the North China Plain. *Palaeogeography, Palaeoclimatology, Palaeoecology* **546**, 109691. <https://doi.org/10.1016/j.palaeo.2020.109691>.
- Xiao, G.Q., Pan, Q., Zhao, Q.Y., Yin, Q.Z., Chen, R.S., Ao, H., Li, X.X., Zhu, Z.M., 2021. Early Pleistocene integration of the Yellow River II: evidence from the Plio-Pleistocene sedimentary record of the Fenwei Basin. *Palaeogeography, Palaeoclimatology, Palaeoecology* **557**, 110550. <https://doi.org/10.1016/j.palaeo.2021.110550>.
- Xiong, J.G., Zhang, H.P., Zhao, X.D., Liu, Q.R., Li, Y.L., Zhang, P.Z., 2021. Origin of the youngest Cenozoic aeolian deposits in the southeastern Chinese Loess Plateau. *Palaeogeography, Palaeoclimatology, Palaeoecology* **561**, 110080. <https://doi.org/10.1016/j.palaeo.2020.110080>.
- Xiong, J.G., Liu, Y.M., Zhang, P.Z., Deng, C.L., Picotti, V., Wang, W.T., Zhang, K., *et al.*, 2022. Entrenchment of the Yellow River since the late Miocene under changing tectonics and climate. *Geomorphology* **416**, 108428. <https://doi.org/10.1016/j.geomorph.2022.108428>.
- Xue, C., Zhou, Y., Wang, G., 2003. Reviews of the Yellow River delta superlobes since 700 BC. *Marine Geology & Quaternary Geology* **23**, 23–29. [in Chinese with English abstract]
- Yang, J.D., Li, G.J., Dai, Y., Rao, W.B., Ji, J.F., 2009. Isotopic evidences for provenances of loess of the Chinese Loess Plateau. *Earth Science Frontiers* **16**, 195–206. [in Chinese with English abstract]
- Yang, J.L., Yuan, H.F., Hu, Y.Z., Wang, F., 2022. Significance of sedimentary provenance reconstruction based on borehole records of the North China Plain for the evolution of the Yellow River. *Geomorphology* **401**, 108077. <https://doi.org/10.1016/j.geomorph.2021.108077>.
- Yang, S.Y., Jiang, S.Y., Ling, H.F., Xia, X.P., Sun, M., Wang, D.J., 2007. Sr-Nd isotopic compositions of the Changjiang sediments: implications for tracing sediment sources. *Science in China Series D: Earth Sciences* **50**, 1556–1565.
- Yao, Z., Shi, X., Qiao, S., Liu, Q., Kandasamy, S., Liu, J., Liu, Y., Fang, X., Gao, J., Dou, Y., 2017. Persistent effects of the Yellow River on the Chinese marginal seas began at least ~880 ka ago. *Scientific Reports* **7**, 2827. <https://doi.org/10.1038/s41598-017-03140-x>.
- Yi, L., Deng, C.L., Tian, L.Z., Xu, X.Y., Jiang, X.Y., Qiang, X.K., Qin, H.F., *et al.*, 2016. Plio-Pleistocene evolution of Bohai Basin (East Asia): demise of Bohai Paleolake and transition to marine environment. *Scientific Reports* **6**, 29403. <https://doi.org/10.1038/srep29403>.
- Zhang, J., Wan, S.M., Clift, P.D., Huang, J., Yu, Z.J., Zhang, K.D., Mei, X., *et al.*, 2019. History of Yellow River and Yangtze River delivering sediment to the Yellow Sea since 3.5 Ma: tectonic or climate forcing? *Quaternary Science Reviews* **216**, 74–88.
- Zhang, W.L., Zhang, T., Song, C.H., Erwin, A., Mao, Z.Q., Fang, Y.H., Lu, Y., *et al.*, 2017. Termination of fluvial-alluvial sedimentation in the Xining Basin, NE Tibetan Plateau, and its subsequent geomorphic evolution. *Geomorphology* **297**, 86–99.
- Zheng, H.B., Huang, X.T., Ji, J.L., Liu, R., Zeng, Q.Y., Jiang, F.C., 2007. Ultra-high rates of loess sedimentation at Zhengzhou since Stage 7: implication for the Yellow River erosion of the Sanmen Gorge. *Geomorphology* **85**, 131–142.